Microstructure and abrasive wear resistance in the Miller test of a martensitic Fe-C alloy with V and W carbides

Grzegorz Tęcza

AGH University of Krakow, Faculty of Foundry Engineering, Kraków, Poland
tecza@agh.edu.pl

(Received 05 November 2025; Accepted 08 June 2026)

Abstract

A very popular material used for parts and components of machines operating under abrasive wear is cast alloyed steel with medium and high carbon content, which ensures sufficient hardness, and with the addition of elements such as Cr, Mn, Si, Ni, Mo. To improve the abrasive wear resistance of the tested alloys, carbide-forming elements such as vanadium were introduced in the amount of about 18 wt.% during melting. One melt, in which the total carbon content ranged from 3.4 to 3.9 wt.%, additionally contained 4.5 wt.% W. The measured hardness of the tested samples in the alloy with a carbon content of 3.4 wt% and the addition of 17.7 wt% V and 4.5 wt% W, the as-cast was approximately 535 HV and increased to approximately 665 HV after quenching. The highest hardness was obtained for an alloy containing 3.9 wt% C and 17.9 wt% V. In the as-cast state, the hardness of this alloy was 850 HV and increased to 950 HV after quenching from a temperature of 880°C and cooling in a 15% of Polihartenol HI polymer solution. The microstructure of test castings was composed of a martensitic matrix with low amounts of retained austenite characterized by the presence of lamellar carbides with a spherical cross-section, evenly distributed in the alloy matrix. In the majority of cases, those were M_2C carbides, though in alloys with vanadium and tungsten, complex carbides of the $(V,W)_xC_y$ type were also observed to occur. The highest resistance to abrasive wear of approximately 950 HV was obtained in a martensitic alloy with 17.9 wt% V+0.1 wt% W, quenched from a temperature of 880°C and cooled in a 15% of Polihartenol HI polymer solution. Its weight loss was two times lower than the weight loss of the reference cast GX70CrMnSiNiMo2 steel.

Keywords: Abrasive Wear, Martensitic Alloy, Microstructure, Vanadium Carbides, Heat Treatment, Hardness

Introduction

Progress in numerous branches of industry, to mention only the energy industry, mining and aggregate processing, has greatly increased the demand for thick-walled castings of machine parts and components made of alloys resistant to abrasive wear. Mining and materials processing as well as the energy industry are among those sectors that show the greatest demand for castings of this type. Therefore, cast martensitic alloy steel is nearly always associated with the production of rings and balls operating in the grinding units of coal mills. The basic chemical composition of an alloy is not always sufficient to generate the required and satisfactory wear resistance, especially when this alloy should withstand the complex wear processes, which occur during its operation and are due to, among others, variable loads and abrasion. Modification of the chemical composition of currently used cast steels by adding carbide-forming elements has a positive effect on both alloy hardness and abrasive wear resistance. Pure wear through mechanical action is a rare case. It is usually accompanied by temperature- and corrosion-related effects. What we observe under real conditions is not one but many different co-existing wear mechanisms, though the dominant one can always be identified.

Abrasive wear represents approximately 80-90% of all types of wear. Castings used in the energy, mining or aggregate processing industries most often operate under the conditions of metal-non-metal friction, and abrasive wear occurs when the abrasive slides accross the surface of a solid body [1–8].

The wear behavior of materials depends on so many factors of so complex nature means that for many years certain studies have become dominant in the development of abrasion-resistant materials with attention focused on certain research trends. Analysis of the literature on the abrasive wear of metals and their alloys indicates that current research is primarily devoted to the development of several technologies improving the abrasion resistance of materials. The most popular and most frequently developed alloy resistant to abrasive wear is cast high-manganese Hadfield steel, in which the improvement in abrasion resistance is achieved, e.g. by the use of a specially selected heat treatment [9,10].

In traditional cast tool steels and cast irons, various types of carbides, of both primary and secondary nature, are produced, where the elements forming primary carbides are added in small amounts and act rather as modifiers. In such alloys, the resistance to abrasive wear is mainly provided by the secondary carbides, which are fine and scarce in number, and precipitate in the solid state after heat treatment. For this reason, further improvements in the heat treatment parameters are so important for the enhancement of the wear resistance of materials [11–15].

Another way to improve abrasion resistance is by producing top layers that harden only the surface of the casting, leaving the core malleable. It is proposed to produce such layers directly on castings in the casting mold [16–18], and to apply protective coatings, e.g. by surface remelting [19,20], or to make such layers by other physical and chemical methods on finished castings [21–24].

A relatively new development in the production of abrasion-resistant castings is the manufacture of composites or making castings with abrasion-resistant composite zones by the Self-Propagating High-Temperature Synthesis. The essence of the latter invention consists in the formation of carbides in some specific zones of the casting as a result of reaction by generating high temperature in the alloy and carbides synthesis from a mixture of powders [25–28].

The next method to obtain a composite structure and high abrasion resistance involves casting two-phase or multi-phase alloys, including iron alloys and tool steel, where the alloy matrix is reinforced with carbides, nitrides or other ceramic particles, which are introduced into the liquid metal in the form of powder. The use of the most commonly added TiC carbides, which are introduced during melting and casting of steel, is justified by their good absorption in liquid steel, high hardness and stability of particles [29–38].

The methods and developments in the materials engineering of abrasion resistant Fe-C alloys presented above are complex, time-consuming and expensive, and, moreover, require additional equipment, additional materials as well as human skill and effort. An equally good solution is the one that allows obtaining high abrasion resistance parameters within the entire casting volume. Compared to the presented modern technologies, the method is faster, easier and cheaper. The authors propose some means for the production of primary carbides in the metallurgical process and the addition of carbide-forming elements to the alloy, which after heat treatment will form secondary carbides. This technology ensures that primary carbides, which provide high wear resistance, are evenly distributed in the alloy matrix, which can additionally be precipitation-strengthened during heat treatment. This enables the production of durable, abrasion-resistant structural components. In previous studies [39–44] on the properties

of cast austenitic steel enriched with the additions of vanadium, titanium and niobium, the authors discussed changes in the microstructure and abrasive wear resistance determined in the Miller test. In all the examined cases, a favorable microstructure was produced in the tested alloys, and in the Miller abrasion resistance tests, at least two times higher resistance to abrasive wear was obtained compared to the reference cast steel. Cast Fe-C alloys with carbides evenly distributed in the matrix provide high abrasion resistance, although, as shown, the plasticity of cast steel suffers a significant drop and the impact strength decreases even twice [41].

Figure 1 compares the smallest weight losses in samples of the alloys with different content of various additives and carbide-forming elements, tested so far by the authors in a 16-hour Miller test (ASTM G75-07). Cast chromium-nickel austenitic steel with the addition of titanium is definitely the material offering the lowest rate of wear, but the obtained results should be referred to the percent content of carbide-forming additives, which will be the subject of a separate study.

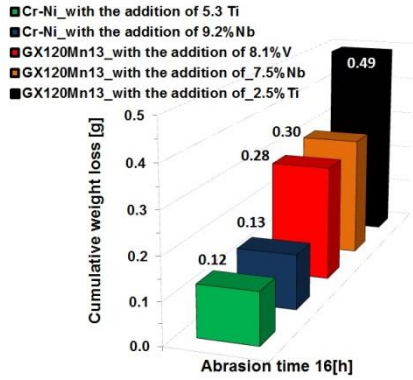

Figure 1. *Comparison of the wear behavior of austenitic alloys tested by the author*

Materials and Methods

Based on the results obtained so far for the alloys with an austenitic matrix, it can be concluded that adding carbide-forming elements to the alloy always tends to increase the matrix hardness, and in the wear tests, favorable results with at least several dozen percent higher abrasion resistance compared to the reference cast steels have been obtained. This prompted the author to conduct similar experiments on alloys with a martensitic matrix. The use of casting as a manufacturing method allows the production of a large amount of carbides, the quantity of which becomes limited by the castability of the alloy [39-45]. The chemical composition of the tested alloys was selected in such a way as to obtain, after solidification and carbides formation from the carbide-forming elements, the chemical composition of the alloy matrix corresponding to cast steel with medium and/or high carbon content, ensuring a sufficiently high hardness of the martensitic matrix. Additionally, the composition included elements such as Cr, Mn, Si, Ni, Mo, which provide sufficient hardenability to thick-walled castings. The tested cast steel was melted in a laboratory induction furnace, Balzers VSG-02, manufactured by Balzers, Germany, provided with a crucible of 1kg capacity. The charge consisted of cast GX70CrMnSiNiMo2 steel scrap and pig iron of known chemical composition. The chemical composition additionally included alloy additives, such as metallic chromium, low-carbon Fe-Mn85, electrolytic nickel, Fe-Si65 and Fe-Mo60, all to a mass of approximately 900g. The entire charge was loaded into the crucible and after melting and stirring, the metal was heated to a temperature of approximately 1600°C, the molten steel was deoxidized with Al added in the amount of 1g/1kg

of steel. After deoxidizing the steel, carbide-forming elements in the form of Fe-V90 and Fe-W90 ferroalloys were added in portions, keeping the temperature of the liquid steel as constant as possible. The metal prepared in this way was held in the furnace for 5 minutes to dissolve alloy additives and reach a pouring temperature of approximately 1550-1560°C. Shortly before pouring the ceramic molds, which were heated to a temperature of about 200°C, the metal was deoxidized with Fe-Ca-Si introduced in the amount of 1g/1kg of steel. In this way, "Y" type test castings with a wall thickness of 25 mm, a length of 70 mm and a weight of approximately 900g were produced. Figure 2 shows the test casting and indicates the way in which samples were cut out. The samples were next used for the heat treatment and wear tests, and for the microstructural examinations.

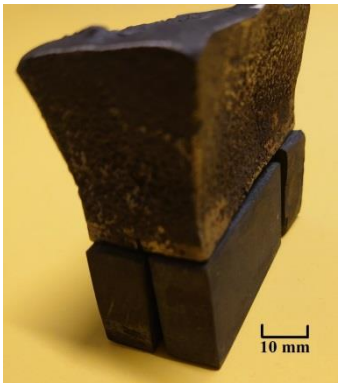

Figure 2. *"Y" type test casting and a method of cutting out the samples*

Chemical analysis of the tested alloys was carried out under industrial conditions using a Spectro Maxx LMF04 spectrometer (Spectro, Kieve, Germany). Additionally, the content of carbide-forming elements was confirmed by the examinations carried out with a Spectro Midex energy dispersive X-ray fluorescence spectrometer (Spectro, Kieve, Germany). Table 1 shows the chemical composition of the tested alloys.

Table 1. *Chemical composition of the tested alloys*

Alloy designation	**Chemical Composition [wt.%]**											
	C	**Mn**	**Si**	**P**	**S**	**Cr**	**Ni**	**V**	**W**	**Mo**	**Ti**	**Al**
P_2	3.4	0.9	0.7	0.06	0.03	1.6	0.02	**17.7**	**4.5**	0.01	0.03	0.02
P_3	3.9	1.1	0.7	0.06	0.04	0.1	0.02	**17.9**	**0.1**	0.01	0.02	0.02

Based on the results of the chemical analysis of the composition of the produced test ingots, it was found that the obtained alloys contained from 3.4 to 3.9 wt.% C, from 0.9 to 1.1 wt.% Mn and 0.7 wt.% Si, which should be sufficient to provide the required hardenability. Additionally, to further improve the hardenability, chromium in the amount of 1.6 wt.% was added to alloy P2. Nickel at the level of 0.02 wt.%, as well as molybdenum and titanium at the level of 0.01-0.05 wt.% were acting as microadditives with only an insignificant effect on the hardenability of the tested alloys and their hardness after quenching. The content of vanadium in the tested alloys it was about 18 wt.%, and ddditionally, 4.5 wt.% W was added to the one alloy to improve its wear resistance.

The hardness of the tested samples, as-cast and after heat treatment, was measured with a Vickers hardness tester (Werkstoffpruefmaschinen, Leipzig, Germany) under a standard load

of 30kg. The results of hardness measurements were presented as independent results. The mean value was not calculated because differences in the obtained hardness values clearly indicated the structural and chemical homogeneity of the alloy.

The microhardness of both alloy matrix and produced carbides was determined by the low-force Vickers hardness measurements according to the method specified in PN-EN-ISO 6507-1:2018, (Leitz Durimet, Wetzlar, Germany) under a load of 100g.

The microstructure of the tested alloys was examined under a Neophot 32 (Carl Zeiss Jena, Hövelhof, Germany) light microscope equipped with a camera for digital image recording.

The heat treatment was performed in a laboratory chamber muffle furnace, model FCF75HM (Czylok, Jastrzębie Zdrój, Poland). Samples with a wall thickness of 25 mm were heated to 880, 920 and 1050°C and annealed for 40 min. followed by cooling in various media. The OH-120M quenching oil (NAFTOCHEM Sp. z o. o., Kraków Poland) and a 15% aqueous solution of Polihartenol HI spolymer (Proimp, Rzeszów, Poland) was used. After hardening, all samples were stress-relieved at a temperature of 200°C. The heat treatment parameters and the hardness values obtained in individual measurements are compared in Table 2.

Microstructural analysis was also performed with a JEOL, JSM-5500LV scanning electron microscope (made in Tokyo, Japan). The microscope was equipped with an EDS detector from Oxford Instruments (made in Abingdon, UK), which enabled chemical analysis of the alloy matrix and carbides visible on metallographic sections. For the examined areas, two qualitative analyses were performed – the first analysis in the form of an EDS energy spectrum and the second one showing chemical composition in atomic percentage. This data analysis allowed determining the type of carbides obtained.

Phases present in the tested samples were identified with a Kristalloflex 4H (Siemens, Munich, Germany) X-ray diffractometer from Siemens using the characteristic Cu radiation (Kα = 0.154 nm) with a step size of 0.052 theta/1 s.

The specimens with the highest hardness after heat treatment were selected for further wear tests. The wear rate was determined in a Miller machine that complies to the ASTM G75 Standard and allows comparing the rate of wear in specimens with different hardness values. Figure 3 shows a schematic diagram of the machine used in Miller test.

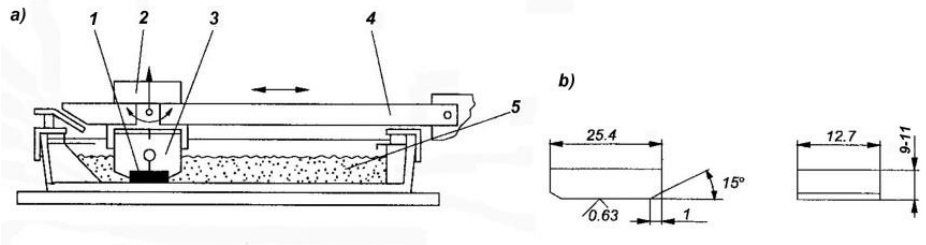

Figure 3. *Schematic diagram of the abrasion testing device (a): 1; specimen, 2; weight, 3; specimen holder, 4; holder arm, and 5; abrasive. (b) dimensions of the specimen tested for abrasive wear [42,44]*

The test involves sliding four specimens, which are mounted and loaded in the handles of the device and move in a reciprocating motion for a specified time in an abrasive environment. Abrasion resistance is determined from the obtained differences in wear rate. Performing tests by the same procedure and under the same conditions allowed the author to compare the currently obtained results with his earlier results and with the results obtained by other researchers [39–49], the latter was, however, possible only when the tests were conducted under

identical conditions of abrasion and all test parameters were kept constant and repeatable. The most important parameters that affect the obtained results include the specimen dimensions , which are 25.4x12.7x9-11 mm, a constant load of 22.2N and an abrasive medium in the form of a suspension composed of water and silicon carbide in a 50/50g ratio. Silicon carbide with a grain size of 53-73 μm was used to prepare the test suspension. The test time and the number of cycles performed are also extremely important. Two tests were performed for each set of specimens, each test including four four-hour abrasion cycles. After each cycle, the specimen was weighed with an accuracy of 0.001g. Based on the obtained changes in the mass of each specimen, the mean value was calculated, the wear curves were plotted and compared with the wear of the reference sample. However, considering the fact that other researchers often do not provide accurate data on the conditions of the experiment, the author could only compare the obtained results with his own previous studies carried out by the Miller test.

The wear values obtained for the tested specimens were compared with the wear of a reference specimen made of cast GX70CrMnSiNiMo2 alloy tool steel, which is used for coal grinding sets in coal-fired power plants. The cast steel composition included 0.7 wt.% C, 1.0 wt.% Mn, 0.5 wt.% Si, 1.8 wt.% Cr, 0.6% Ni and 0.4 wt.% Mo. The cast steel was heat-treated (toughening) to an average hardness of 400 HV. The surfaces of all specimens after the abrasion test were macroscopically compared with the reference specimen and, based on the obtained results, the wear mechanism was determined. An analysis was conducted and the surfaces of the samples after wear testing were compared using the KEYENCE Digital Microscope VHX-7000 series with advanced image analysis. The wear profiles of the samples were compared by observing them in full depth of field, their surface roughness was assessed, and based on these observations, the mechanism of their wear was determined.

Test results and discussion

Heat treatment and hardness

The study presents the results of a research on the microstructure of the tested alloys obtained after casting and heat treatment. The results of hardness measurements and abrasive wear resistance tests carried out on the martensitic alloys with vanadium and tungsten carbides produced in a metallurgical process are presented. The heat treatment parameters and measured hardness average values are compared in Table 2.

Table 2. *Heat treatment parameters and hardness of the tested samples*

Alloy designation	Heat treatment	Average HV ±δ
P2 (17.7 wt.% V+4.5 wt.% W)	As-cast	534 ±6
	880°C/40 min./15% HI polymer	578 ±12
	880°C/40 min./oil	545 ±2
	920°C/40 min./15% HI polymer	626 ±7
	1150°C/40 min./15% HI polymer	667 ±2
P3 (17.9 wt.% V+0.1 wt.% W)	As-cast	856 ±12
	880°C/40 min./15% HI polymer	951 ±15
	880°C/40 min./oil	873 ±3
	920°C/40 min./15% HI polymer	874 ±9
	1150°C/40 min./15% HI polymer	868 ±9

The alloy with 3.4 wt.% C and the addition of 17.7 wt.% V and 4.5 wt.% W, designated as P2, was characterized by much good hardness. In the as-cast condition, its hardness was approximately 534 HV and with the increase in quenching temperature, samples quenched from

a temperature of 1150°C reached the hardness of approximately 667 HV. In this alloy, the increase in hardness with the increase in quenching temperature was caused by the dissolution of carbides in the matrix, increasing with the austenitizing temperature, which is of crucial importance for the improvement in hardenability. The highest hardness was obtained for alloy P3 with a carbon content of 3.9 wt.% and 17.9 wt.% V. In the as-cast state, the hardness value was as high as 856 HV and increased further to 951 HV after quenching from a temperature of 880°C with cooling in a 15% HI polymer solution. For this chemical composition, the increase in quenching temperature had no significant impact on the hardness value. The maximum hardness measured was obtained for the alloy quenched from a temperature of 880°C with cooling in a 15% HI polymer solution. It amounted to 1020 HV, but the sample cracked before the annealing operation. As a result of fracture and stress relief annealing, the hardness dropped to approximately 951 HV. Additionally, for all tested alloys, samples hardened in an aqueous polymer solution had slightly higher hardness compared to samples hardened in oil. The small scatter of the hardness values proves the structural and chemical homogeneity of the tested alloys and a uniform distribution of carbide precipitates in the alloy matrix. For the tested alloys, the measured hardness of visible carbides ranged from 2140 HV0.1 to 2690 HV0.1. The alloy matrix hardness was comparable to the matrix hardness measured with a Vickers hardness tester under a load of 30kg and ranged from 880 to 960 HV 0.1. Figure 4 shows an example of the microstructure obtained in alloy P3 with a carbon content of 3.9 wt.% and 17.9 wt.% V; microhardness imprints and respective values are visible in the tested areas.

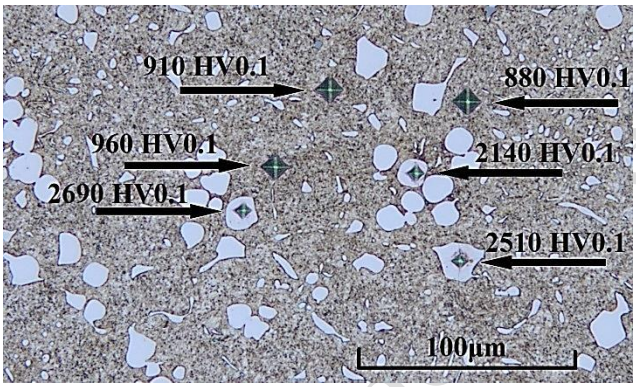

Figure 4. *Example of the microstructure obtained in alloy P3 (17.9 wt.% V+0.1 wt.% W) with hardness measurements in the tested areas, etched with nital*

Microstructure

Figures 5 and 6 show the characteristic microstructures obtained in the unetched and etched state, respectively, in alloy P2 containing 3.4 wt.% C and the addition of 17.7 wt.% V and 4.5 wt.% W. Some attention deserves the morphology of carbides obtained in this alloy. The examinations carried out by light microscopy (Figures 5 and 6) and scanning microscopy (Figures 7 and 8) as well as the chemical analysis of the composition of visible carbides (Tables 3 and 4) allow concluding that, apart from lamellar carbides in the predominant part with a spherical cross-section evenly distributed in the martensitic matrix of the alloy (Figures 5a, 6a and 7), a small amount of eutectic carbides (Figures 6a, b and 7.) also occurs in the areas of retained austenite, the presence of which has been confirmed by X-ray examinations of phases present in the alloy (Figure 9). Most of the retained austenite was observed in the areas of eutectic carbides (Figures 6a, b and 7), which are the primary interdendritic spaces. Vanadium in the presence of tungsten forms complex carbides of the $(V,W)_xC_y$ of the VC type. Examples of the chemical composition of these carbides are given in Table 3, point 2 and Table 4, point 1. They mainly contain vanadium up to 40 at% and a small amount of tungsten, i.e. up to 1.8

at%. In alloy P2 with the addition of 4.5 wt.% W, few, single dispersion carbides enriched in tungsten were observed to occur in the interdendritic spaces (Figure 7, point 1 and Table 3, point 1). They contain primarily vanadium in an amount of up to about 30 at% and tungsten in an amount of up to about 5 at%.

A completely different structure, especially as regards carbide morphology, was obtained in alloy P3 with vanadium. Examinations by light microscopy (Figures 10 and 11) and by scanning microscopy (Figures 13 and 14) as well as chemical analysis of the composition of visible carbides (Tables 5 and 6) allow concluding that the microstructure of this alloy consists of a martensitic matrix with oval and spherical carbides, which are evenly distributed in this matrix (Figures 10a and 11a). The observed carbides are most frequently of the VC type. Examples of their chemical composition are given in Table 5, point 1. They contain primarily vanadium in an amount of up to 46 at% and small amounts (up to 0.1 at%) of other carbide-forming elements. Additionally, few, small clusters of complex eutectic carbides of the $(V,Fe)_xC_y$ type VC, were observed on metallographic sections in the primary interdendritic spaces (Figure 14, Table 6, point 1). Besides vanadium in an amount of approximately 20 at%, they additionally contained Fe in an amount of approximately 16 at%. In alloy P3, no retained austenite was observed on metallographic sections (Figure 11c), although X-ray tests have indicated its presence (Figure 12). Owing to this microstructure, the obtained hardness of this alloy is the highest of all alloys tested so far and, on average, approaches 950HV.

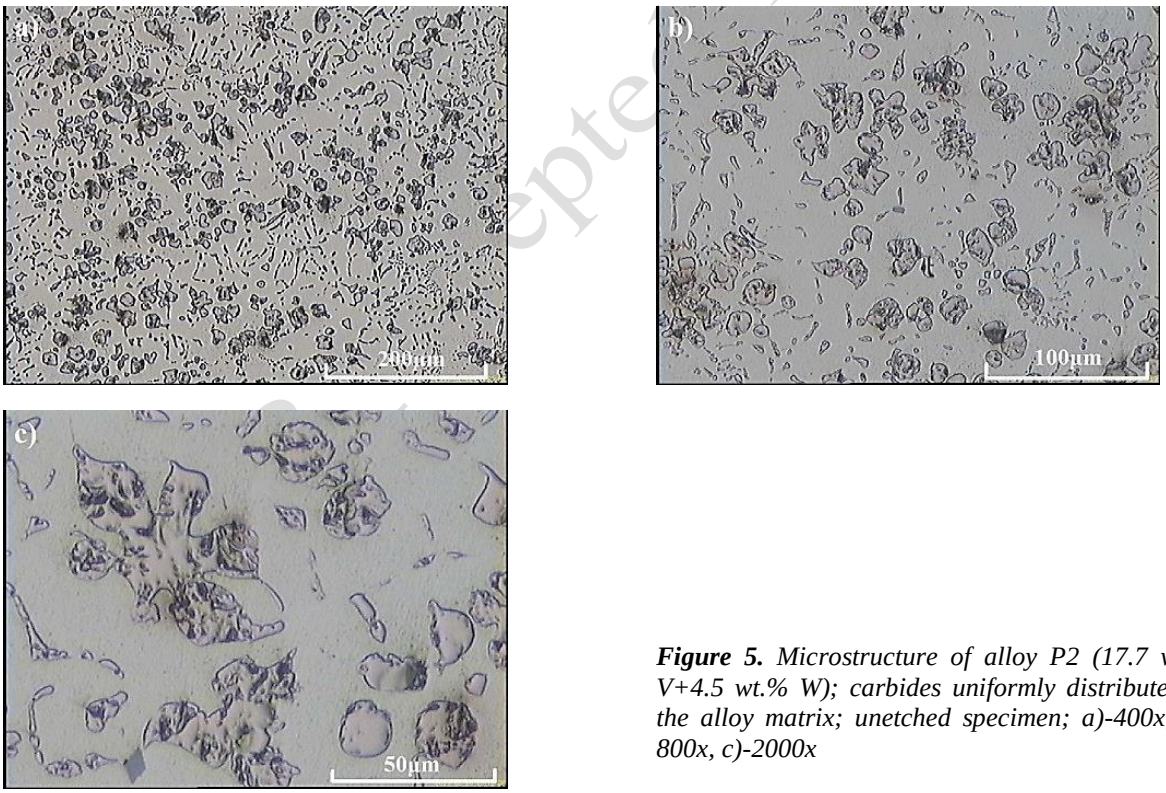

Figure 5. *Microstructure of alloy P2 (17.7 wt.% V+4.5 wt.% W); carbides uniformly distributed in the alloy matrix; unetched specimen; a)-400x, b)-800x, c)-2000x*

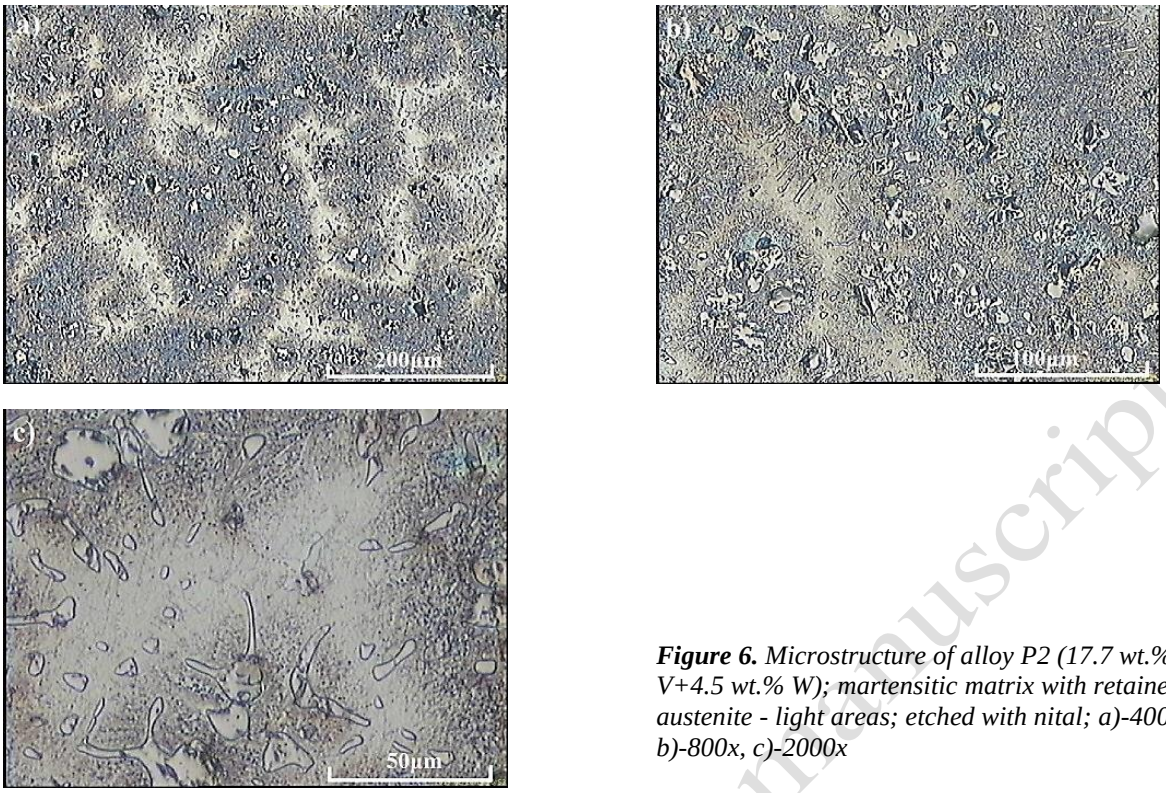

Figure 6. *Microstructure of alloy P2 (17.7 wt.% V+4.5 wt.% W); martensitic matrix with retained austenite - light areas; etched with nital; a)-400x, b)-800x, c)-2000x*

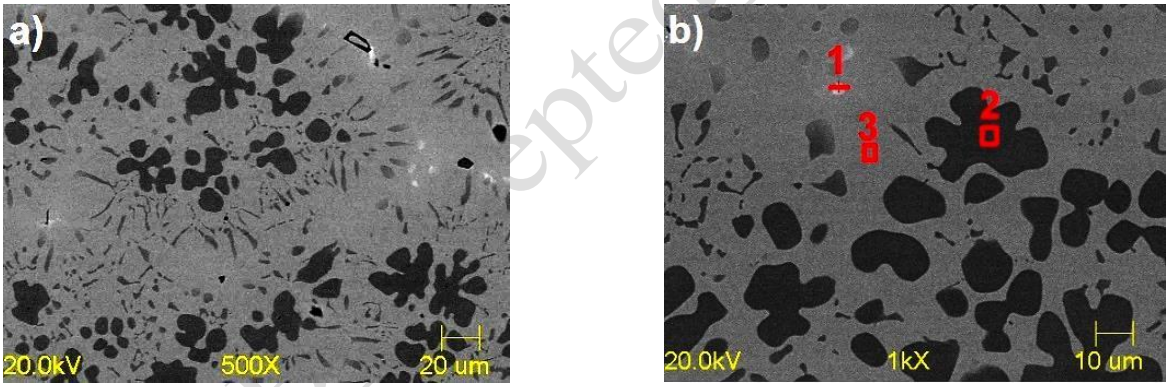

Figure 7. *Scanning image of alloy P2 (17.7 wt.% V+4.5 wt.% W; a)-oval and lamellar carbides evenly distributed in the alloy matrix, b)-marked locations of analysis*

Table 3*. Chemical composition of areas at points 1, 2 and 3, Figure 7*

Location of analysis	[at%]									
	C	**Si**	**Ti**	**V**	**Cr**	**Mn**	**Fe**	**Mo**	**W**	**Total**
point 1	58.4	–	0.1	30.7	2.2	–	3.4	0.1	5.1	100.0
point 2	56.6	–	0.1	41.0	0.3	–	0.9	0.1	1.0	100.0
point 3	9.9	1.4	0.2	3.2	1.4	0.4	82.7	0.2	0.6	100.0

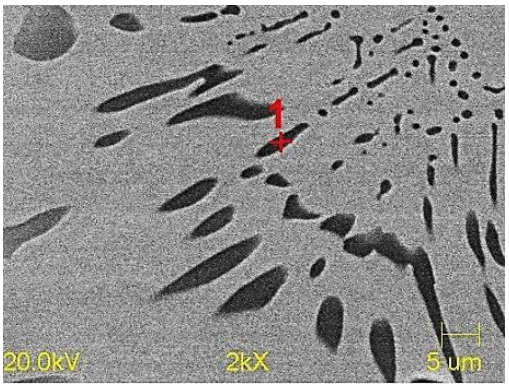

Figure 8. Scanning image of alloy P2 (17.7 wt.% V+4.5 wt.% W); lamellar and eutectic carbides in the alloy matrix

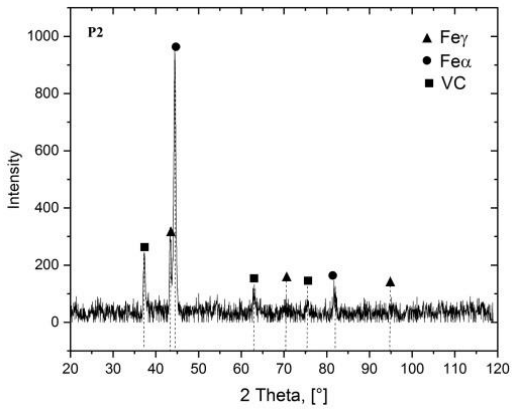

Figure 9. *X-ray diffractogram of alloy P2 (17.7 wt.% V+4.5 wt.% W)*

Table 4. *Chemical composition of carbides at point 1, Figure 8*

Location of analysis	[at%]								
	C	**Ti**	**V**	**Cr**	**Mn**	**Fe**	**Mo**	**W**	**Total**
point 1	59.1	0.1	34.4	0.8	0.1	3.6	0.1	1.8	100.0

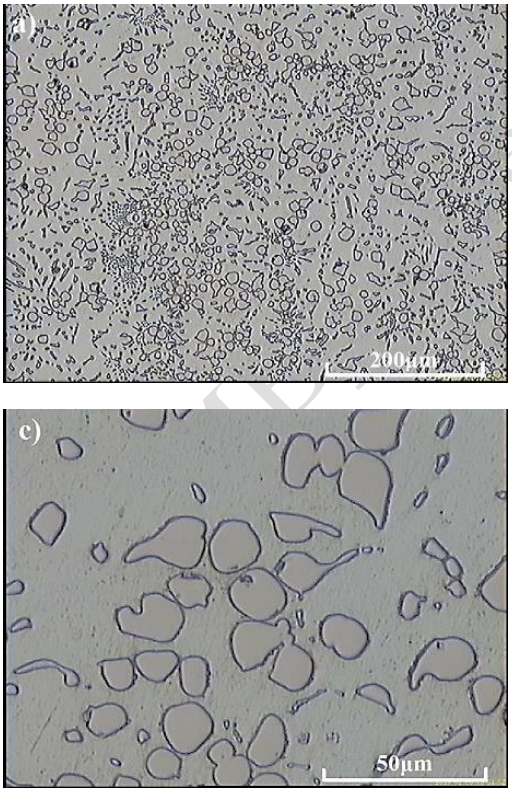

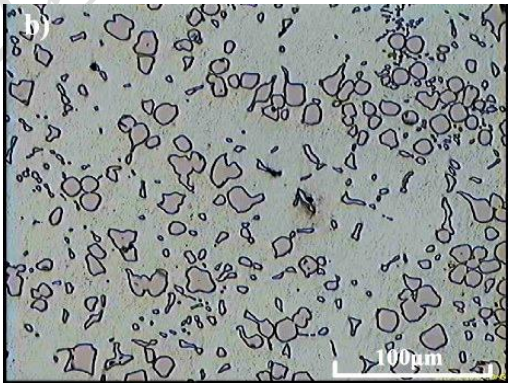

Figure 10. *Microstructure of alloy P3 (17.9 wt.% V+0.1 wt.% W); carbides evenly distributed in the alloy matrix; unetched specimen; a)-400x, b)-800x, c)-2000x*

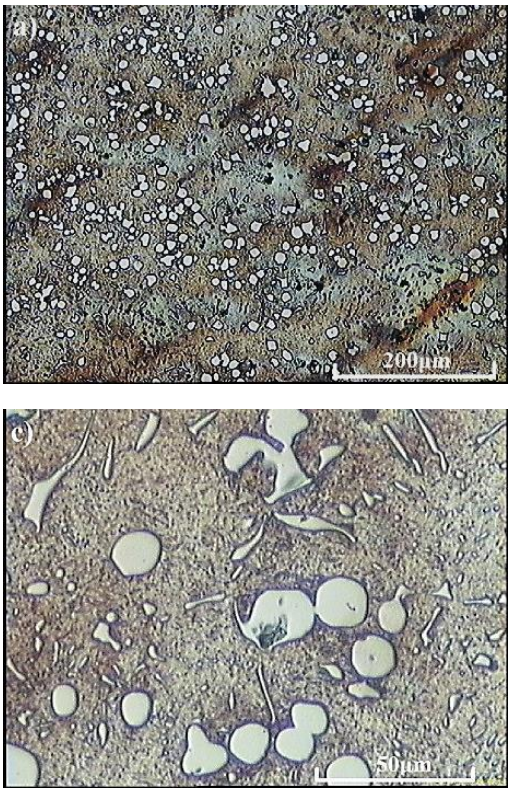

Figure 11. *Microstructure of alloy P3 (17.9 wt.% V+0.1 wt.% W); martensitic alloy matrix without retained austenite; etched with nital; a)-400x, b)-800x,c)-2000x*

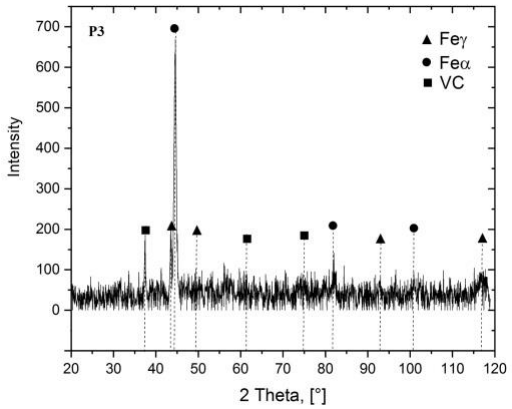

Figure 12. *X-ray diffractogram of alloy P3 (17.9 wt.% V+0.1 wt.% W)*

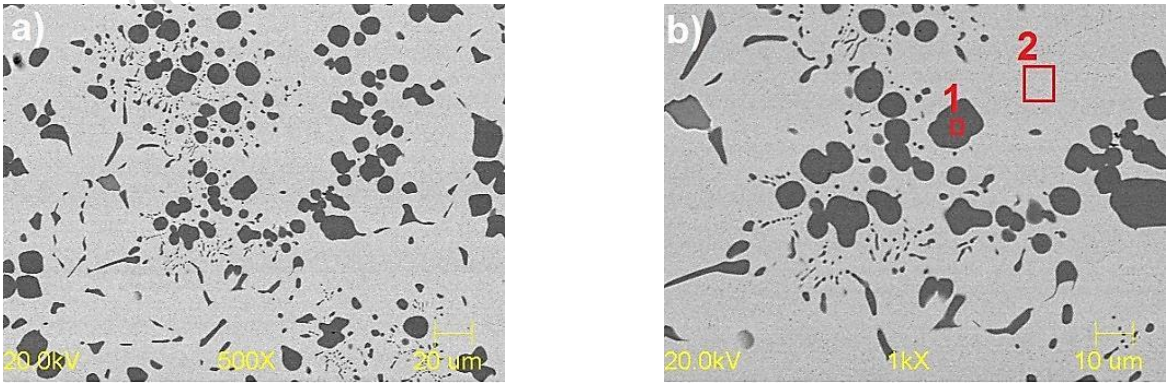

Figure 13. *Scanning image of alloy P3 (17.9 wt.% V+0.1 wt.% W); a)-oval and spherical carbides evenly distributed in the alloy matrix, b)-marked locations of analysis*

Table 5. *Chemical composition of areas at points 1 and 2, Figure 13*

Location of analysis	[at%]									
	C	**Si**	**Ti**	**V**	**Cr**	**Mn**	**Fe**	**Mo**	**W**	**Total**
point 1	52.7	–	0.1	46.0	–	0.1	0.9	0.1	0.1	100.0
point 2	12.6	1.6	0.2	1.4	–	0.5	83.1	0.1	0.5	100.0

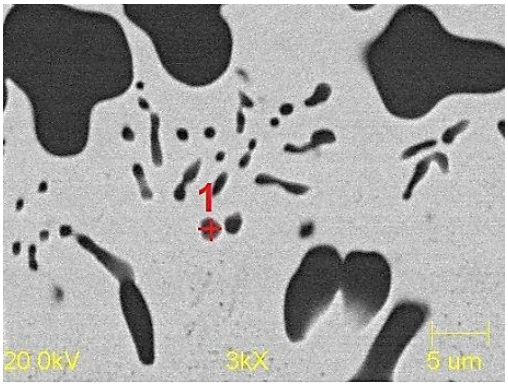

Figure 14. *Scanning image of alloy P3 (17.9 wt.% V+0.1 wt.% W); eutectic and lamellar carbides in the alloy matrix*

Table 6. *Chemical composition of carbides at point 1, Figure 14*

Location of analysis	[at%]									
	C	**Si**	**Ti**	**V**	**Cr**	**Mn**	**Fe**	**Mo**	**W**	**Total**
point 1	62.3	0.3	–	20.5	–	0.3	16.4	0.1	0.1	100.0

Wear Resistance

Samples with the highest matrix hardness were subjected to Miller abrasion tests. Tests included alloy P2 (17.7 wt.% V+4.5 wt.% W), quenched from a temperature of 1150°C and cooled in a 15% HI polymer solution to a hardness of approximately 665 HV, and alloy P3 (17.9 wt.% V+0.1 wt.% W), quenched from a temperature of 880°C and cooled in a 15% HI polymer solution to a hardness of approximately 950 HV. The reference material to compare the test results was cast GX70CrMnSiNiMo2 alloy steel, subjected to standard heat treatment to an average hardness of 400 HV.

Based on individual weight losses, the total weight loss of the specimens during the test was calculated. The results were used to plot a graph of the cumulative weight loss of the specimens as a function of the abrasion time, shown in Figure 15.

The obtained values of the total weight loss show the highest resistance to abrasive wear of martensitic alloy P3 (17.9 wt.% V+0.1 wt.% W), quenched from a temperature of 880°C with cooling in a 15% HI polymer solution to a hardness of approximately 950 HV. Its weight loss of 0.262g/16h was two times lower than the weight loss of the reference cast GX70CrMnSiNiMo2 steel, where the wear rate was the highest and amounted to 0.525g/16h. The wear rate of alloy P2 (17.7 wt.% V + 4.5 wt.% W) increased slightly with the addition of vanadium and tungsten (compared to alloy P3), which was due to a lower hardness of the alloy matrix compared to alloy P3 and was caused by depletion of the matrix in carbon when the vanadium and tungsten carbides were formed.

The linear run of the wear traces obtained for the reference GX70CrMnSiNiMo2 alloy and alloy P2 (17.7 wt.% V + 4.5 wt.% W) proves their uniform wear over 16 hour cycle. A different run of the wear traces was observed in alloy P3 (17.9 wt.% V+0.1 wt.% W). A gradual flattening of the line can be seen, which indicates that wear is slowly stabilizing over time. As the matrix wear proceeds, the carbides are exposed and confer an exceptionally high abrasion resistance to the tested material. It can be expected that the carbides will chip off at a certain stage of wear, but as a result of progress in the matrix wear, new carbides will be exposed, the balance will be re-established, and the wear will stabilize at an even level.

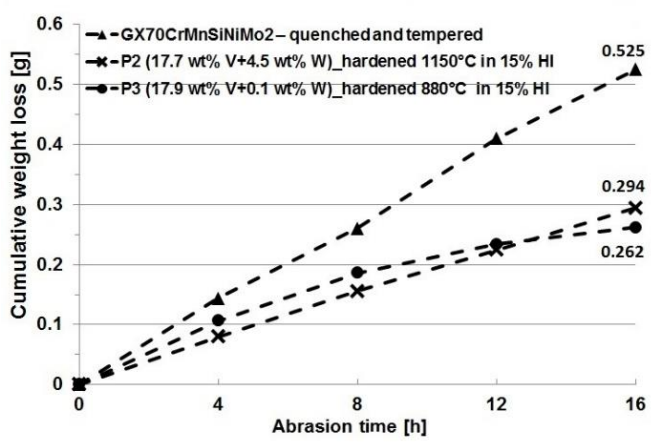

Figure 15. *Cumulative weight loss of specimens of the tested alloys as a function of abrasion time*

Figure 16 shows a macroscopic image of the surface of specimens tested for abrasion resistance. The most uniform wear in all the studies of the abrasion resistance presented so far was obtained by the author for the group of martensitic alloys with vanadium. All tested specimens with a high content of carbides in the alloy matrix had an even and slightly rough surface and, as a result of matrix wear, carbides exposed from the alloy matrix were visible on the surface. On the surface of the specimens subjected to a 16-hour abrasion test, no chipping of carbides from the abraded surfaces or the formation of scratches or furrows was observed.

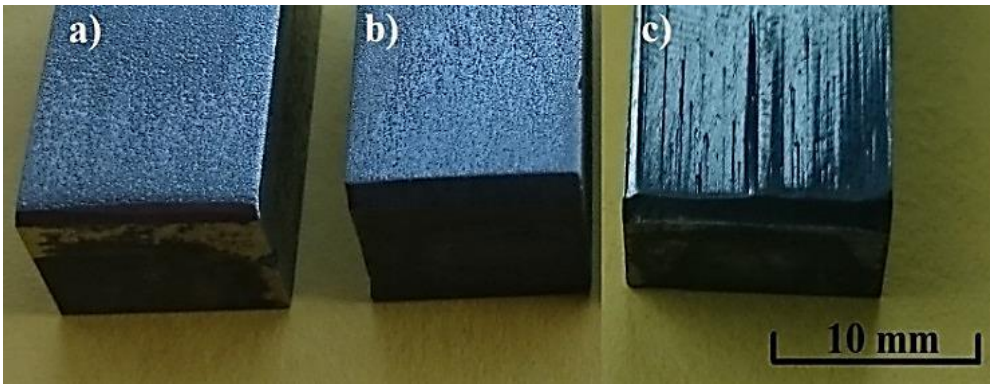

Figure 16. *The surface of specimens after abrasion test: a) – martensitic alloy P2 with the addition of 17.7 wt.% V + 4.5 wt.% W, b)-martensitic alloy P3 with the addition of 17.9 wt.% V+0.1 wt.% W, c)-reference specimen cast GX70CrMnSiNiMo2 steel*

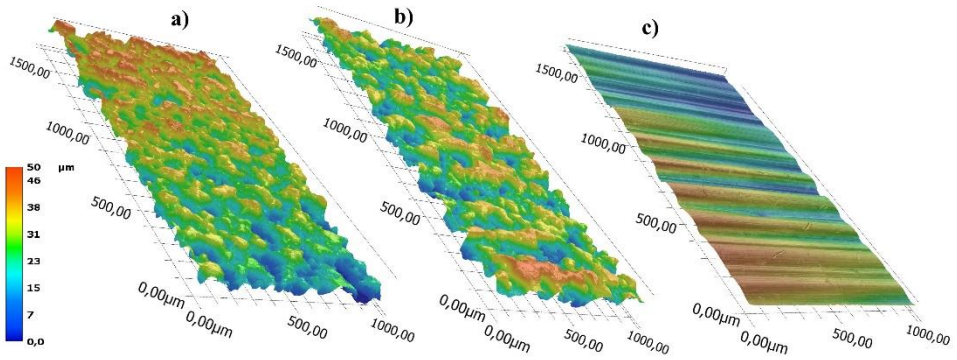

Figure 17. Comparison of wear surface profiles obtained in the Miller test: a) – martensitic alloy P2 with the addition of 17.7 wt.% V + 4.5 wt.% W, b)-martensitic alloy P3 with the addition of 17.9 wt.% V+0.1 wt.% W, c)-reference specimen cast GX70CrMnSiNiMo2 steel

Samples with the addition of V and W tested in a 16-hour abrasion test were characterized by the surfaces even and homogeneous, with well-visible carbides protruding from the alloy matrix. No scratches or grooves were formed on the abraded surfaces and there was no sign of carbide chipping from these surfaces. Due to the high hardness of the matrix and protruding carbide particles, the wear was uniform, and SiC particles were not penetrating into the abraded surfaces. The differences in the height of the wear profiles visible in Figure 17, where the protruding particles form local peaks and the worn out matrix forms depressions, confirm this mechanism.

Conclusions

High carbon content in martensitic alloys and the presence of carbide-forming elements with a high affinity for carbon give these alloys exceptional hardness and precipitation-hardened matrix. The favorable morphology of oval carbides, which are evenly distributed in the alloy matrix, also has a beneficial effect on the fracture toughness of castings. Combined together, these properties result in an equally high abrasion resistance of the alloys, and the following conclusions can be drawn from the conducted tests:

1. The microstructure of the tested alloys consists of a martensitic matrix with carbides evenly distributed in this matrix.
2. The obtained carbides are in prevailing part characterized by an oval cross-section.
3. A small amount of retained austenite was observed in the areas of eutectic carbides.
4. Lamellar eutectic carbides were observed to occur in primary interdendritic spaces in the areas of retained austenite.
5. In the alloy with vanadium, the most common were VC-type carbides.
6. Vanadium in the presence of tungsten forms complex carbides of the $(V,W)_xC_y$ type.
7. The highest hardness of approximately 950 HV was obtained for an alloy with the addition of 17.9 wt.% V + 0.1 wt.% W, quenched from 880°C and cooled in a 15% polymer solution.

8. The formation of vanadium and tungsten carbides in the martensitic matrix increases the abrasive wear resistance even twice and makes the sample wear uniform.

Acknowledgments: The article was prepared under the contract 16.16.170.654/B02.

Funding: This research received no external funding.

Conflicts of Interest: The author declares no conflict of interest.

Data availability: The data are available on request from the corresponding author.

References

[1] L.A. Dobrzański, Materiały inżynierskie i projektowanie materiałowe (Engineering materials and materials design), WTN, Warszawa, 2006.
[2] M. Blicharski, Inżynieria Materiałowa – stal (Materials engineering – steel), WNT, Warszawa, 2004.
[3] S. Lamb, CASTI Handbook Stainless Steels and Nickel Alloys, CASTI Publishing Inc, Canada, 2001.
[4] Volume 1: Metals Handbook, Properties and Selection: Irons, Steels, and High-Performance Alloys, 10th ed., ASM International, 1990.
[5] J. Głownia, Metallurgy and Technology of Steel Castings, Bentham Science Publishers, Sharhah, 2017.
[6] J. Głownia, Charakterystyka stali na odlewy (Characteristics of steel for castings), Wydawnictwa AGH, Kraków, 2010.
[7] J. Głownia, Odlewy ze stali stopowej – zastosowanie (Alloy steel castings –applications), FotoBit, Kraków, 2002.
[8] Z. Stradomski, Mikrostruktura w zagadnieniach zużycia staliw trudnościeralnych (The role of microstructure in the wear behavior of abrasion-resistant cast steels), Wydawnictwo Politechniki Częstochowskiej , Częstochowa, 2010.
[9] M. Dziubek, M. Rutkowska-Gorczyca, D. Grygier, The effect of the austenitisation temperaturefor the two-stage heat treatment of high-manganesesteels on its wear resistance under abrasiveconditions, Tribologia 305 (2023) 19–29. https://doi.org/10.5604/01.3001.0053.9426.
[10] M. Dziubek, M. Rutkowska-Gorczyca, W. Dudziński, D. Grygier, Investigation into changes of microstructure and abrasive wear resistance occurring in high manganese steel X120Mn12 during isothermal annealing and re-austenitisation process, Materials 15 (2022). https://doi.org/10.3390/MA15072622.
[11] M. Maher, I. Iraola-Arregui, H. Ben Youcef, B. Rhouta, V. Trabadelo, Microstructural evolution of heat-treated Cr–W–V–Mo steels: effect of core-shell carbides and secondary precipitation on their abrasion resistance, Journal of Materials Research and Technology 24 (2023) 27–38. https://doi.org/10.1016/J.JMRT.2023.02.201.
[12] H. Pourasiabi, J.D. Gates, Effects of chromium carbide volume fraction on high-stress abrasion performance of NbC-bearing high chromium white cast irons, Wear 498–499 (2022). https://doi.org/10.1016/J.WEAR.2022.204312.
[13] M. Pokusová, I. Berta, Ľ. Šooš, Abrasion resistance of as-cast high-chromium cast iron, Scientific Proceedings Faculty of Mechanical Engineering 22 (2014) 75–80. https://doi.org/10.2478/STU-2014-0013.
[14] M. Hirose, K. Yamamoto, H. Miyahara, K. Sakata, K. Ogi, Abrasion behavior of high Cr-V-Nb cast iron, Key Eng Mater 457 (2011) 243–248. https://doi.org/10.4028/WWW.SCIENTIFIC.NET/KEM.457.243.
[15] M. Wang, D. Ma, Z. Liu, J. Zhou, H. Chi, J. Dia, Effect of Nb on segregation, primary carbides and toughness of H13 steel, Acta Metallurgica Sinica 50 (2014) 285–293.
[16] Ł. Szymański, E. Olejnik, T. Tokarski, P. Kurtyka, D. Drożyński, S. Żymankowska-Kumon, Reactive casting coatings for obtaining in situ composite layers based on Fe alloys, Surf Coat Technol 350 (2018) 346–358. https://doi.org/10.1016/J.SURFCOAT.2018.06.085.
[17] Ł. Szymański, E. Olejnik, J.J. Sobczak, M. Szala, P. Kurtyka, T. Tokarski, A. Janas, Dry sliding, slurry abrasion and cavitation erosion of composite layers reinforced by TiC fabricated in situ in cast steel and gray cast iron, J Mater Process Technol 308 (2022). https://doi.org/10.1016/J.JMATPROTEC.2022.117688.
[18] Ł. Szymański, E. Olejnik, J.J. Sobczak, T. Tokarski, Improvement of TiC/Fe in situ composite layer formation on surface of Fe-based castings, Mater Lett 309 (2022). https://doi.org/10.1016/J.MATLET.2021.131399.
[19] Y. Bao, L. Huang, Q. An, R. Zhang, L. Geng, X. Ma, G. Tang, H. Zhang, Wear resistance of TiB/Ti composite coating fabricated by TIG cladding using Ti-TiB2 cored wire, Surf Coat Technol 474 (2023). https://doi.org/10.1016/J.SURFCOAT.2023.130086.

[20] Y. Wei, A. Feng, C. Chen, D. Shang, X. Pan, J. Xue, Effects of laser remelting on microstructure, wear resistance, and impact resistance of laser-clad Inconel625-Ni/WC composite coating on Cr12MoV steel, Coatings 13 (2023). https://doi.org/10.3390/COATINGS13061039.
[21] T. Dong, X. Wang, F. Li, Y. Zhu, X. Fu, Study on the wear resistance of Ni-Co-ZrO2 composite coatings with different ZrO2 nanoparticle concentrations prepared using electrodeposition on the micro-surface of spindle hook teeth, Metals (Basel) 13 (2023). https://doi.org/10.3390/MET13071251.
[22] H. Ding, Y. Cao, K. Hua, Y. Tong, N. Li, L. Sun, X. Li, H. Wu, H. Wang, Fretting wear resistance at ambient and elevated temperatures of 316 stainless steel improved by laser cladding with Co-based alloy/WC/CaF2 composite coating, Opt Laser Technol 163 (2023). https://doi.org/10.1016/J.OPTLASTEC.2023.109428.
[23] M.Ye. Skyba, M.S. Stechyshyn, V.P. Oleksandrenko, N.S. Mashovets, Yu.M. Bilyk, Wear resistance of composite electrolytic coatings, Problems of Tribology 27 (2022) 6–13. https://doi.org/10.31891/2079-1372-2022-103-1-6-14.
[24] E. Fominov, M. Aliev, E. Fisunova, C. Shuchev, N. Metelkova, Influence of coatings based on Zr and Ti on the wear resistance of cemented carbide tools when turning transport machines' parts from structural steels, E3S Web of Conferences 389 (2023). https://doi.org/10.1051/E3SCONF/202338905029.
[25] E. Olejnik, A. Janas, A. Kolbus, G. Sikora, The composition of reaction substrates for TiC carbides synthesis and its influence on the thickness of iron casting composite layer, Archives of Foundry Engineering 11 (2011) 165–168.
[26] E. Olejnik, T. Tokarski, G. Sikora, S. Sobula, W. Maziarz, Ł. Szymański, B. Grabowska, The effect of Fe addition on fragmentation phenomena, macrostructure, microstructure, and hardness of TiC-Fe local reinforcements fabricated in situ in steel casting, Metall Mater Trans A Phys Metall Mater Sci 50 (2019) 975–986. https://doi.org/10.1007/S11661-018-4992-6/FIG.S/12.
[27] S. Sobula, E. Olejnik, T. Tokarski, Wear resistance of TiC reinforced cast steel matrix composite, Archives of Foundry Engineering 17 (2017) 143–146. https://doi.org/10.1515/AFE-2017-0026.
[28] N. Razumov, D. Masaylo, M. Kovalev, E. Volokitina, A. Mazeeva, A. Popovich, Structure and wear resistance of composite TiC-NiMo coating produced by L-DED on Ti-6Al-4V substrate, Metals (Basel) 13 (2023). https://doi.org/10.3390/MET13121925.
[29] A.K. Srivastava, K. Das, Microstructural and Mechanical Characterization of in Situ TiC and (Ti,W)C-Reinforced High Manganese Austenitic Steel Matrix Composites, Materials Science and Engineering: A 516 (2009) 1–6. https://doi.org/10.1016/J.MSEA.2009.04.041.
[30] K. Das, T.K. Bandyopadhyay, S. Das, A review on the various synthesis routes of TiC reinforced ferrous based composites, J Mater Sci 37 (2002) 3881–3892. https://doi.org/10.1023/A:1019699205003/METRICS.
[31] Ö.N. Doğan, J.A. Hawk, J.H. Tylczak, Wear of cast chromium steels with TiC reinforcement, Wear 250 (2001) 462–469. https://doi.org/10.1016/S0043-1648(01)00635-4.
[32] S. Kajiwara, D. Liu, T. Kikuchi, N. Shinya, Remarkable improvement of shape memory effect in Fe-Mn-Si based shape memory alloys by producing NbC precipitates, Scr Mater 44 (2001) 2809–2814. https://doi.org/10.1016/S1359-6462(01)00978-2.
[33] Y. Yazawa, T. Furuhara, T. Maki, Effect of matrix recrystallization on morphology, crystallography and coarsening behavior of vanadium carbide in austenite, Acta Mater 52 (2004) 3727–3736. https://doi.org/10.1016/J.ACTAMAT.2004.04.027.
[34] Ö.N. Doğan, J.A. Hawk, K.K. Schrems, TiC-reinforced cast Cr steels, J Mater Eng Perform 15 (2006) 320–327. https://doi.org/10.1361/105994906X108585/METRICS.
[35] W. Jing, W. Yisan, D. Yichao, Reaction synthesis of Fe–(Ti,V)C composites, J Mater Process Technol 197 (2008) 54–58. https://doi.org/10.1016/J.JMATPROTEC.2007.06.016.
[36] I.Y. Kim, B.J. Choi, Y.J. Kim, Y.Z. Lee, Friction and wear behavior of titanium matrix (TiB + TiC) composites, Wear 271 (2011) 1962–1965. https://doi.org/10.1016/J.WEAR.2010.12.072.
[37] Z. Liu, M. Zhou, Y. Jiang, Z. Wang, The impact abrasive wear resistance and mechanical properties of in situ NbC-reinforced H13 steel composites, J Mater Eng Perform 33 (2023) 9879–9892. https://doi.org/10.1007/S11665-023-08645-3/FIG.S/14.
[38] V.G. Efremenko, K. Shimizu, A.P. Cheiliakh, T. V. Kozarevs'ka, Y.G. Chabak, H. Hara, K. Kusumoto, Abrasive wear resistance of spheroidal vanadium carbide cast irons, Journal of Friction and Wear 34 (2013) 466–474. https://doi.org/10.3103/S1068366613060068/METRICS.
[39] G. Tęcza, J. Głownia, Resistance to abrasive wear and volume fraction of carbides in cast high-manganese austenitic steel with composite structure, Archives of Foundry Engineering 15 (2015) 129–133. https://doi.org/10.1515/AFE-2015-0092.
[40] G. Tęcza, A. Garbacz-Klempka, Microstructure of cast high-manganese steel containing titanium, Archives of Foundry Engineering 16 (2016) 163–168. https://doi.org/10.1515/AFE-2016-0103.
[41] G. Tęcza, R. Zapała, Changes in impact strength and abrasive wear resistance of cast high manganese steel due to the formation of primary titanium carbides, Archives of Foundry Engineering 18 (2018) 119–122. https://doi.org/10.24425/118823.

[42] G. Tęcza, Changes in abrasive wear resistance during Miller test of high-manganese cast steel with niobium carbides formed in the alloy matrix, Applied Sciences 11 (2021) 4794. https://doi.org/10.3390/APP11114794.
[43] G. Tęcza, Changes in abrasive wear resistance during miller test of Cr-Ni cast steel with Ti carbides formed in the alloy matrix, Archives of Foundry Engineering 2021 (2021) 110–115. https://doi.org/10.24425/afe.2021.139758.
[44] G. Tęcza, Changes in microstructure and abrasion resistance during miller test of Hadfield high-manganese cast steel after the formation of vanadium carbides in alloy matrix, Materials 15 (2022). https://doi.org/10.3390/MA15031021.
[45] G. Tęcza, Changes in the microstructure and abrasion resistance of tool cast steel after the formation of titanium carbides in the alloy matrix, Archives of Foundry Engineering 23 (2023) 173–180. https://doi.org/10.24425/AFE.2023.148961.
[46] B. Kalandyk, R. Zapała, The abrasive wear behaviour of alloy cast steel in SiC-water slurry, Archives of Foundry Engineering 9 (2009) 91–94.
[47] B. Kalandyk, R. Zapała, Effect of high-manganese cast steel strain hardening on the abrasion wear resistance in a mixture of SiC and water, Archives of Foundry Engineering; 2013; No 4 13 (2013) 63–66. https://doi.org/10.2478/AFE-2013-0083.
[48] J. Kasinska, B. Kalandyk, Effects of rare earth metal addition on wear resistance of chromium-molybdenum cast steel, Archives of Foundry Engineering 17 (2017) 63–68. https://doi.org/10.1515/afe-2017-0092.
[49] B. Kalandyk, Wear resistance of 18%Cr-9%Ni steel used for cast parts of pumps operating in corrosive – erosive environments, Archives of Metallurgy and Materials 58 (2013) 841–844. https://doi.org/10.2478/AMM-2013-0083.

List of figures captions

List of tables captions